In search of the RNA world on Mars

Angel Mojarro[1*], Lin Jin[2], Jack W. Szostak[2], James W. Head III[3], and Maria T. Zuber[1]

[1]Department of Earth, Atmospheric and Planetary Sciences, Massachusetts Institute of Technology, Cambridge, Massachusetts.

[2]Department of Molecular Biology, and Center for Computational and Integrative Biology, Massachusetts General Hospital, Boston, Massachusetts.

[3]Department of Earth, Environmental and Planetary Sciences, Brown University, Providence, Rhode Island.

*Address correspondence to:

Angel Mojarro

Massachusetts Institute of Technology

77 Massachusetts Ave, Room E25-647

Cambridge, MA, 02139

E-mail: mojarro@mit.edu

Abstract:

Advances in origins of life research and prebiotic chemistry suggest that life as we know it may have emerged from an earlier RNA World. However, it has been difficult to reconcile the conditions used in laboratory experiments with real-world geochemical environments that may have existed on the early Earth and hosted the origin(s) of life. This challenge is in part due to geologic resurfacing and recycling that have erased the overwhelming majority of the Earth's prebiotic history. We therefore propose that Mars, a planet frozen in time, comprised of many surfaces that have remained relatively unchanged since their formation >4 Gya, is the best alternative to search for environments consistent with geochemical requirements imposed by the RNA world. In this study we synthesize *in situ* and orbital observations of Mars and modeling of its early atmosphere into solutions containing a range of pHs and concentrations of prebiotically relevant metals (Fe^{2+}, Mg^{2+}, and Mn^{2+}), spanning various candidate aqueous environments. We then experimentally determine RNA degradation kinetics due to metal-catalyzed hydrolysis and evaluate whether early Mars could have been permissive towards the accumulation of long-lived RNA polymers. Our results indicate that a Mg^{2+}-rich basalt sourcing metals to a slightly acidic (pH 5.4) aqueous environment mediates the slowest rates of metal-catalyzed RNA hydrolysis, though geologic evidence and modeling of basalt weathering suggest that aquifers on Mars would be near neutral (pH ~7). Moreover, oxidizing conditions on Mars have major consequences regarding the availability oxygen-sensitive prebiotic metals (i.e., Fe^{2+} and Mn^{2+}) very early in its history due to increased RNA degradation rates and precipitation. Overall, 1) low pH better preserves RNA than basic conditions at high concentrations; 2) acidic to neutral pH environments with Fe^{2+} or Mn^{2+} will hydrolyze more RNA; and 3) alkaline environments with Mg^{2+} dramatically hydrolyze more RNA.

Key words: RNA world, Origins of Life, Mars

1. Introduction

The origins of life can best be understood as a series of plausible steps culminating in the emergence of a "self-sustaining chemical system capable of Darwinian evolution" (NASA Astrobiology). However, life as we know it is a highly complex collection of molecular machinery and genetic information. The central dogma of molecular biology stipulates that deoxyribonucleic acid (DNA) makes ribonucleic acid (RNA) via transcription, RNA makes protein via translation, and information cannot be transferred backwards from proteins to nucleic acids (Crick, 1970). Fundamentally, neither DNA, RNA, nor proteins can exist without the others as they do today. Nevertheless, this dilemma belies the fact that the capability of translating information between dissimilar polymers (e.g., polynucleotides to polypeptides) is mediated by the ribosome, an RNA enzyme (Cech, 2000). This is significant because the ribosome is arguably an evolutionary anachronism from a period where RNA polymers acted as both enzymes (protein) and information storage (DNA) (Petrov et al., 2015). Additional discoveries of structural and regulatory RNA molecules (Breaker, 2012) suggest that life may have emerged from an earlier RNA world dominated by ribozymes (e.g., the ribosome) (Gilbert, 1986) and ribonucleotide-containing molecules (e.g., adenosine triphosphate - ATP) (Hernández-Morales et al., 2019) catalyzing reactions and mediating a protometabolism.

Under the RNA world scenario, abiotic synthesis of simple RNA molecules from common molecular feedstocks in geologically relevant environments (e.g., Patel et al., 2015) would have given rise to self-assembling protocellular systems (Joyce and Szostak, 2018). Thereafter increasingly complex RNA polymers capable of both hereditary storage and

autocatalysis would precede the DNA-RNA-protein world (Bernhardt, 2012). To test the RNA world hypothesis investigators have experimentally demonstrated: 1) abiotic RNA synthesis (e.g., Powner et al., 2009); 2) non-enzymatic RNA replication (Adamala and Szostak, 2013; Jin et al., 2018); 3) self-assembly of protocell membranes and membrane replication (Schrum et al., 2010); 4) directed evolution and fitness landscapes yielding persistent RNA motifs (Jimenez et al., 2013) and functional ribozymes (Voytek and Joyce, 2007); and 5) the co-synthesis of RNA, amino acids, and lipids (Patel et al., 2015).

Although strides in prebiotic chemistry have demonstrated the viability of an origin of life via the RNA world, a longstanding criticism is that RNA is inherently unstable due to the presence of a nucleophilic 2'-hydroxyl group which readily catalyzes cleavage of the 5',3'-phosphodiester bond (Li and Breaker, 1999). Because of this characteristic, RNA is deemed an ephemeral molecule that is unlikely to accumulate, functionalize, and precipitate life in a prebiotic world. Researchers have therefore directed efforts towards determining particular conditions or cofactors which can stabilize RNA in real-world environments. Experimental work suggests: 1) RNA is most chemically stable between pH 4 – 5 (Bernhardt and Tate, 2012; Oivanen et al., 1998) and near 0 °C (Kua and Bada, 2011; Levy and Miller, 1998); 2) metal cofactors such as Fe^{2+}, Mg^{2+}, and Mn^{2+} facilitate the folding of RNA polymers into stable secondary and tertiary structures (Bowman et al., 2012; Laing et al., 1994; Petrov et al., 2012); 3) copolymers such as polypeptides and polysaccharides can favor specific polynucleotide conformations, resulting in persistent structures and vice-versa (Runnels et al., 2018); and 4) folding of many RNA sequences decreases rapidly above 30 °C (Moulton et al., 2000).

Still, it has been difficult to confidently determine the dynamic environments that could have existed on the Hadean Earth and hosted the origin of life. This challenge is in part due to

geologic resurfacing and recycling that have erased the overwhelming majority of the Earth's prebiotic history (Marchi et al., 2014). Nevertheless, we can speculate that the likeliest time interval for the origin of life on Earth is best constrained by the accretion of the first continents following a Moon-forming impact 4.5 – 4.3 Gya (Monteux et al., 2016) and the earliest putative biosignatures ~3.7 Gya (Nutman et al., 2016). Given this consideration, the best alternative is to search for environments consistent with RNA stability on Mars, a planet frozen in time, preserving primordial surfaces which have remained relatively unchanged since they formed >4 Gya (Hartmann and Neukum, 2001). Reminiscent of the Hadean epoch on Earth (Nisbet and Sleep, 2001), the Noachian period on Mars is characterized by meteoritic bombardment and punctuated aqueous activity resulting in extensive ground water circulation (Ehlmann et al., 2011), valley networks (Fassett and Head, 2011), and long-lived lacustrine environments (Goudge et al., 2015, 2012; Grotzinger et al., 2014). Some researchers would argue that life began on Mars and was transported to the Earth around the timing of the earliest biosignatures ~3.7 Gya (Benner and Kim, 2015). That is, non-sterilizing lithological exchange between Mars and Earth from impact ejecta produced during the presumed Late-Heavy Bombardment period (Boehnke and Harrison, 2016; Gomes et al., 2005) may have transported viable microbes between planets resulting in ancestrally related life (Gladman et al., 1996; Weiss, 2000).

The case for an origin of life on Mars relies on prebiotic environments that are inferred to be analogous to environments on Earth, common molecular feedstocks (including cometary sources) (Callahan et al., 2011), and plausible reactive pathways predicted on Earth that are applicable on Mars (e.g., Ritson et al., 2018) which may have resulted in parallel events in accordance to the RNA world hypothesis (Benner and Kim, 2015). This notion is further supported by *in situ* detection of boron (Gasda et al., 2017), which is considered crucial to

stabilize ribose in the formose reaction (Furukawa and Kakegawa, 2017), experimental work that predicts higher phosphate bioavailability on Mars (Adcock et al., 2013), and the detection of clays (Ehlmann et al., 2011) that have been demonstrated to assist in non-enzymatic RNA polymerization (Ferris, 2006). This Mars origin of life hypothesis suggests that past or present Martian life may have utilized known building blocks (e.g., nucleic acids, sugars, amino acids) and closely resembled life as we know it. Moreover, if life exists on Mars today, it could theoretically be detected by means of nucleic acid (DNA and RNA) sequencing (Carr et al., 2017; Mojarro et al., 2019). Assuming that viable RNA was being delivered to Mars via unspecified sources (e.g., cometary or *in situ* synthesis) to UV-shielded aqueous environments (Cockell et al., 2000), here we investigate whether early Mars was permissive towards the accumulation of long-lived RNA polymers. We anticipate our findings could provide insight into potential mechanisms, environments, and requirements necessary for sustaining an RNA world on the early Earth.

2. Materials and Methods

2.1. Approach

The surface of Mars displays evidence for alternating climate regimes at regional-to-global magnitudes that have evolved on variable time scales not dissimilar to the Earth (McLennan et al., 2019). In general, early Mars contained a broad range of geochemical environments (e.g., acidic to alkaline) primarily influenced by redox chemistry. In this study, we synthesize *in situ* and orbital observations and modeling of the early Martian atmosphere in order to extrapolate representative solutions containing a range of pHs and metals analogous to various candidate aqueous environments on Mars. Below we detail our experimental design, which involves

incubating an RNA-DNA chimeric oligomer (simply referred to as the RNA oligomer) to quantify the hydrolysis rate of the 5',3'-phosphodiester bond at a single ribonucleotide within the aforementioned solutions. The goal of this study is to understand the influence of bedrock composition (e.g., mafic-ultramafic, iron-rich, magnesium-rich, etc.) and subsequent weathering of prebiotically relevant metals (Fe^{2+}, Mg^{2+}, and Mn^{2+}) which have been demonstrated to catalyze hydrolysis (Fedor, 2002), folding (Laing et al., 1994), and translation (Bray et al., 2018) on RNA stability. Furthermore, pH is simultaneously adjusted to reflect the composition of a hypothetical anoxic and CO_2-dominated atmosphere at variable pressures in equilibrium with surface waters, an average acid vent, and alkaline vent (Kua and Bada, 2011). The end result is an analysis of single-stranded RNA stability and degradation kinetics in an array of simulated prebiotic geochemical spaces on Mars.

2.2. RNA oligomer

A hybrid RNA-DNA oligomer, 5'-Cy3-TTT-TTT-rCTT-TTT-TTT-3', was designed to contain one ribonucleotide (r) in between deoxyribonucleotides, allowing us to quantify hydrolysis at a single cleavage site (Figure 1) (Adamala and Szostak, 2013). RNAse free and HPLC-purified oligos were ordered from Integrated DNA Technologies (IDT).

2.3. Relevant observations

Mars Exploration Rover Opportunity: Sedimentary rocks exposed in the Meridiani Planum region (Burns formation) of Mars record alternating periods of acidic groundwater flow (pH ~2 - 4) and desiccation under highly oxidizing conditions (Klingelhofer, 2004; McLennan, 2012; Squyres et al., 2006; Squyres and Knoll, 2005).

Mars Exploration Rover Spirit: Widespread Fe^{3+}-sulfate soils (e.g., jarosite) at Gusev Crater indicate acid-weathering of primarily olivine-rich outcrops in a possible hydrothermal environment (Ming et al., 2008; Yen et al., 2008).

Mars Science Laboratory (MSL) Curiosity: Sedimentary rocks analyzed at Gale Crater (Bradbury-Mount Sharp groups) reflect a long-lived lacustrine environment with circumneutral pH waters and variable redox states as indicated by the presence of manganese oxide (Mn^{2+}) deposits, magnetite-silica facies (Fe^{2+}), and hematite-phyllosilicate facies (Fe^{3+}) (Grotzinger et al., 2015, 2014; Hurowitz et al., 2017; Lanza et al., 2016).

Mars Reconnaissance Orbiter & Mars Express: Crustal Fe-Mg smectites indicate global groundwater circulation (Ehlmann et al., 2011) consistent with recent work suggesting subsurface waters were primarily anoxic, Fe^{2+}-rich, and circumneutral pH which became rapidly acidified due to atmospheric O_2 or photo-oxidation of Fe^{2+} to Fe^{3+} at the Martian surface (Hurowitz et al., 2010). Mg^{2+}-rich carbonate deposits near Nili Fossae indicate neutral to alkaline pH waters likely in contact with a CO_2 atmosphere (Ehlmann et al., 2008). Abundant Late Noachian aqueous surface environments and features, including fluvial valley networks (e.g., Fassett and Head, 2008; Hynek et al., 2010) open-basin lakes (e.g., Fassett and Head, 2008b; Goudge et al., 2012) and closed-basin (endorheic) lakes (e.g., Goudge et al., 2015).

Mars Atmosphere and Volatile Evolution: Isotopic evidence indicates a continuous loss of a ≥0.5 bar CO_2-dominated and increasingly oxidizing atmosphere (Jakosky et al., 2017) since the early Noachian ~4.1 Gya due to erosion by solar wind when the Martian dynamo is thought to have shut down (Lillis et al., 2013).

Atmospheric Modeling: No atmospheric model has been able to resolve liquid water on the early Mars with a faint young sun. Various models have suggested a range of atmospheric

compositions (e.g., H_2, CO_2, H_2O, SO_2, H_2S); however, none has been able to balance counteracting cooling effects of atmospheric density and albedo due to aerosol and cloud formation (e.g., Palumbo et al., 2018; Tian et al., 2010). Due to lower solar luminosity values in early history, recent atmospheric general circulation models (e.g., Forget et al., 2013; Palumbo and Head, 2018; Wordsworth et al., 2013) have found it difficult to maintain the >273 K mean annual temperature (MAT) seemingly required to support a "warm and wet" or "warm and arid" early Mars climate proposed to account for the valley networks interpreted to have transported liquid water on the surface (e.g., Craddock et al., 2003). Instead, these models suggest a "cold and icy" early Mars climate (Head and Marchant, 2014) in which snow and ice were deposited in the uplands, and episodic transient heating events caused melting and runoff to form the valley networks and lakes. Among the candidate transient events proposed are those due to: 1) spin-axis/orbital variations influencing peak annual and seasonal temperatures (Palumbo et al., 2018); 2) volcanic eruptions (e.g., Halevy and Head III, 2014); 3) impact events (e.g., Palumbo and Head, 2018; Segura et al., 2008; Steakley et al., 2019; Turbet et al., 2020); 4) subsurface radiolytic H_2 production and release (e.g., Tarnas et al., 2018); and 5) collision-induced absorption (CIA) temperature amplifications during transient CO_2 and methane release events (e.g., Wordsworth et al., 2017).

2.4. Mars prebiotic geochemical solutions

Given the aforementioned observations, we designed our experiments to simulate environments that are in equilibrium with an anoxic CO_2-dominated atmosphere at variable pressures (10 bar, 0.1 bar, >>0.1 bar) inducing their respective shifts in pH (5.4, 6.7, 8) as calculated by Kua and Bada, 2011. Solutions representing an average acidic vent at pH 3.2 and alkaline vent at pH 9

were also included. Each pH solution contained 0, 2.5, 5, 10, 25, and 50 mM of Fe^{2+}, Mg^{2+}, or Mn^{2+} intended to represent a range of dissolved metal concentrations within the water column, variable weathering, and residence times. Mixtures of Fe^{2+} and Mg^{2+} at 50:50, 20:80, and 80:20 (25 mM total) were included to represent metal concentrations derived from variable bedrock compositions, in particular, 20:80 Fe^{2+}:Mg^{2+} is closest to the average crustal composition on Mars (Mittlefehldt, 1994). A total of 5 pH conditions, 3 metals at 5 concentrations, 3 basalt analogs, and 5 negative controls resulted in 95 unique conditions.

Samples were prepared by mixing stock buffer solutions of 1 M Glycine-HCL (Sigma-Aldrich, 50046) at pH 3.2, 0.5 M MES (Sigma-Aldrich, 76039) at pH 5.4 and 6.7, 1 M Tris pH 8 (Thermo Fisher, AM9849), and 1 M Tris pH 9 (Millipore, 9295-OP) with stock solutions of 0.5 M ammonium iron(II) sulfate hexahydrate (Sigma-Aldrich, 09719), 0.5 M manganese(II) chloride tetrahydrate (Sigma-Aldrich, 63535), or 0.5 M magnesium chloride (Thermo Fisher, AM9530G). A typical RNA incubation consisted of 250 mM buffer, 1 mM EDTA (Thermo Fisher, AM9260G), 0 – 50 mM of metals, and 5 µM of the RNA oligomer in a final 20 µL reaction. All stock solutions were sparged with argon and stored inside an anaerobic glove box (Coy). The atmosphere inside the glove box was N_2 with 2.5 – 3% H_2 and internal circulation through a platinum catalyst maintained residual oxygen levels below 10 ppm. All RNA reactions occurred inside the glove box on a miniPCR mini16 thermocycler (Amplyus, QP-1016-01) kept at 75 °C in order to facilitate rapid RNA degradation.

2.5. RNA degradation quantification

All RNA degradation experiments were quantified via urea polyacrylamide gel electrophoresis (National Diagnostics, EC-830 & EC-840) followed by imaging on a Typhoon 9410 (GE

Healthcare). Two bands were detected representing either the intact 15-mer (5'-Cy3-TTT-TTT-rCTT-TTT-TTT-3') or the residual 7-mer (5'-Cy3-TTT-TTT-rC-3') cleaved at the single ribonucleotide site (Figure 1). Scans were then analyzed with the ImageQuant TL 7.1 software (GE Healthcare).

2.5. RNA degradation kinetics

5 µM of the RNA oligomer was incubated in each of the Mars solutions as described above at 75 ºC (n = 2) inside an anaerobic chamber. 1 µL aliquot time points were taken at 5, 15, 30, 60, and 120 minutes for pH 6.7, 8, and 9 and at 10, 30, 60, 120, and 240 minutes for pH 3.2 and 5.4. Aliquots were added to 25 µL of a kill buffer solution of 8 M Urea, 1x TBE, and 100 mM EDTA. Samples were then removed from the anaerobic chamber and 5 µL of the kill buffer and time point mixture (2 picomols RNA) was taken for gel electrophoresis and quantification. Pseudo-first order reaction kinetics $k_{obs}(h^{-1})$ of RNA hydrolysis were determined with the following relationship, $\ln[p_t] = -kt + \ln[p_o]$ where p_t = percent intact oligo at t = time n and p_o = percent intact oligo at t = 0 (Figure 2).

3. Results

Our experimental results indicate that enhanced RNA hydrolysis occurs due to the presence of metals (i.e., metal-catalyzed hydrolysis) in nearly all pH conditions (Table 1). However, at pH 3.2, increasing metal concentration decreases the rate of degradation (Figure 3). Hydrolysis at pH 3.2 is best mitigated by Mg^{2+} at 50 mM ($k_{obs}(h^{-1})$ = 0.013) followed by Fe^{2+} at 50 mM ($k_{obs}(h^{-1})$ = 0.025) then Mn^{2+} at 50 mM ($k_{obs}(h^{-1})$ = 0.026) relative to the negative control ($k_{obs}(h^{-1})$ = 0.081). Between pH 5.4 and 8, RNA incubations containing Mg^{2+} are generally more stable than those

containing Fe^{2+}. This preference is most apparent in saturation curves fitted to the Michaelis-Menten model for enzyme kinetics (Figure 4) which indicate a stability optimum at pH 5.4 where the maximum rate of RNA hydrolysis in the presence of Mg^{2+} ($k_{max}(h^{-1})$ = 0.0095) is notably lower than for Fe^{2+} ($k_{max}(h^{-1})$ = 0.071). Trends for Mn^{2+} solutions are quantitatively similar to Fe^{2+} between pH 3.2 and 8 (Figure 5, Table 1). At pH 9, we record the most rapid metal-catalyzed hydrolysis rates in our experiments. Michaelis-Menten models show that Fe^{2+} ($k_{max}(h^{-1})$ = 0.61) is more stable than Mg^{2+} ($k_{max}(h^{-1})$ = 0.96) although both Fe^{2+} and Mn^{2+} precipitated out of solution (Figure 4, Table 2). Results for the basalt analog solutions tend towards less overall metal-catalyzed hydrolysis in Mg^{2+}-rich solutions (e.g., forsteritic) over Fe^{2+}-rich solutions (e.g., fayalitic) (Figure 6). A summary of all the results produced in this study is presented in Table 1 and Table 2.

4. Discussion

4.1. Prebiotic metal catalysis

In aqueous solution Mg^{2+}, Fe^{2+}, and Mn^{2+} form a hydrated hexa aquo species ($Mg^{2+}(H_2O)_6$, pK_a = 11.4, $Fe^{2+}(H_2O)_6$, pK_a = 9.6, and $Mn^{2+}(H_2O)_6$, pK_a = 10.6) which polarize first shell water molecules in a tightly packed octahedral geometry (Jackson et al., 2015). Normally, these metal aquo complexes interact with secondary and tertiary RNA structures to neutralize the electrostatic repulsion of negatively charged phosphate groups brought into close proximity, or to increase local rigidity and join distal RNA structures by incorporating phosphate groups into their first coordination shell (Petrov et al., 2012). However, in our experiments, we sought to quantify the effect of metal-catalyzed RNA cleavage by transesterification, which is thought to be analogous to how certain ribozymes (e.g., the hammerhead self-cleaving ribozyme) utilize

metals to stabilize transition states and catalyze cleavage of the 5',3'-phosphodiester bond (Fedor, 2002; Hampel and Cowan, 1997; Johnson-Buck et al., 2011). Namely, 1) acid/base interactions with water result in the activation of the ribose 2'-hydroxyl nucleophile, and 2) first shell phosphate ligands draw electron density and expose phosphorous to nucleophilic attack. Attack of the 2'-hydroxyl on the adjacent phosphate results in formation of a 2'-3' cyclic phosphate terminated oligonucleotide plus a second oligonucleotide product that begins with a 5'-hydroxyl.

Our results reproduce the enhanced RNA degradation rates expected to be associated with each metal's respective acid dissociation constant (pK_a) in solution. Between pH 5.4 and 8, slower rates of metal-catalyzed hydrolysis occur in the presence of Mg^{2+} (pK_a = 11.4) followed interchangeably by Mn^{2+} (pK_a = 10.6) and Fe^{2+} (pK_a = 9.6) (Figure 4, Table 1). Moreover, because of low lying d orbitals, both Fe^{2+} and Mn^{2+} have greater electron withdrawing power (Fe^{2+} = 0.11 e^-) than Mg^{2+} (0.08 e^-) (Okafor et al., 2017) which likely compound the rate of RNA cleavage due to mechanism 2) described above (Hampel and Cowan, 1997). At pH 9, it would appear that slower degradation rates occur in the presence of Fe^{2+} ($k_{max}(h^{-1})$ = 0.61) rather than Mg^{2+} ($k_{max}(h^{-1})$ = 0.96) contrary to our interpretation for pH 5.4 – 8 (Figure 4). Nonetheless, it is known that alkaline Fe^{2+} solutions will begin to form insoluble species such as $Fe(OH)_2$ around pH ~9 (Gayer and Woontner, 1956) that would sequester Fe^{2+} from participating in catalysis. Precipitates were observed for both Fe^{2+} and Mn^{2+} solutions albeit considerably more with Fe^{2+} at pH 9 corroborating interpretations that solubility properties are responsible for the observed differences between Mg^{2+} and Fe^{2+}(Jin et al., 2018). Results for pH 3.2 were unexpected as increasing concentrations of prebiotic metals decreased the rate of hydrolysis (Figure 3) and additional work is required to understand the precise preservation mechanism. However,

300 researchers have proposed that perhaps metal ions can act as Lewis acids which stabilize the 2'-
301 hydroxyl group and prevent nucleophilic attack of phosphorous (Fedor, 2002). Results for the
302 basalt analogs demonstrate greater degradation rates with increasing concentrations of Fe^{2+}
303 relative to Mg^{2+} (Figure 6). This is best observed at pH 6.7 and 8 where 80:20 (20 mM Mg^{2+}: 5
304 mM Fe^{2+}) is mostly Mg^{2+}-dominated then transitions to Fe^{2+}-dominated at 20:80 (5 mM Mg^{2+}:
305 20 mM Fe^{2+}) (Table 1, Figure 6). Metal-catalyzed RNA cleavage at pH 9 for all basalt analogs is
306 inferred to be primarily Mg^{2+}-dominated as Fe^{2+} was observed to precipitate out of solution.
307
308 *4.2. RNA on Mars*
309 Our results demonstrate that RNA stability depends on both metal concentration and pH. While
310 concentrations up to 50 mM were tested here, lower metal concentrations ~1 mM are more
311 geochemically plausible on Earth though estimates on Mars are not well constrained (Catling,
312 1999). Observations from anoxic crater lakes and perennially stratified ferruginous lakes on
313 Earth show that ranges between 0 – 1.5 mM of dissolved Fe^{2+}, Mn^{2+}, or Mg^{2+} are reasonable for
314 a basalt hosted basin (e.g., Bura-Nakić et al., 2009; Busigny et al., 2014; Hongve, 1994; Kling et
315 al., 1989). However, such low values are often at odds with proposed prebiotic chemistries which
316 require 50 - 250 mM of metals for *in situ* RNA synthesis (e.g., 250 mM Fe^{2+} - Patel et al., 2015)
317 or replication (e.g., 50 - 200 mM Mg^{2+} - Szostak, 2012). It is unclear whether such high
318 concentrations of metals would be geochemically reasonable on early Mars, however, periods of
319 wet-dry cycling (e.g., playa environments) or endorheic lakes could conceivably facilitate
320 required concentrations (e.g., Patel et al., 2015). Meanwhile, *in situ* observations on Mars
321 suggest pH regimes ranging from acidic (pH 2 - 4) (e.g., Squyres and Knoll, 2005) to
322 circumneutral (pH ~7) (e.g., Grotzinger et al., 2014,) existed on various locations around the

323 planet. Observations by MAVEN constrain the composition of the early atmosphere to primarily
324 CO_2-dominated at ≥0.5 bars, which accordingly would not considerably acidify surface
325 environments below pH ~6.7 (Kua and Bada, 2011). Modeling of continental weathering of early
326 Earth basalts additionally suggests that waters with high alkalinity would have stabilized pH
327 between 6.6 and 7 under a ~1 bar CO_2 atmosphere (Halevy and Bachan, 2017; Krissansen-Totton
328 et al., 2018). This is important because subsurface basaltic aquifers on Mars would have globally
329 theoretically sustained neutral pH waters as observed at Gale Crater (Grotzinger et al., 2014).
330 Our results indicate that a Mg^{2+}-rich basalt (e.g., McSween, 2002; Mustard et al., 2005)
331 sourcing metals to a slightly acidic (pH 5.4) aqueous environment on Mars would have best
332 supported long-lived single-stranded RNA polymers. Notwithstanding this conclusion, CO_2
333 pressures (10 bar) required to acidify surface waters are not supported by atmospheric models
334 (Forget et al., 2013; Tian et al., 2010) while buffering from a basaltic aquifer would neutralize
335 pH as indicated above. Results from our experiments at pH 6.7 therefore represent the most
336 accurate interpretation of potentially global conditions on Mars (Bibring et al., 2006), or at least
337 those found locally at Gale Crater (Hurowitz et al., 2017). Depending on how early Mars became
338 oxidizing, aqueous environments like Meridiani Planum and Gusev Crater (pH 2 - 4) would
339 accelerate RNA hydrolysis rates at low concentrations as observed at pH 3.2 (Figure 3) while the
340 oxidation of Fe^{2+} to Fe^{3+} would produce a well-known iron species that forms a strong complex
341 with phosphate and leads to the precipitation of RNA (van Roode and Orgel, 1980). This is
342 particularly significant because researchers have proposed that Fe^{2+} may have promoted RNA
343 replication (Jin et al., 2018), folding (Athavale et al., 2012), and novel catalytic activity (Hsiao et
344 al., 2013; Okafor et al., 2017) on Earth prior to the great oxidation event ~2.45 Gya when life
345 would have transitioned to Mg^{2+}.

Most relevant to this study, work on non-enzymatic RNA replication has demonstrated that metal-catalyzed hydrolysis increases the rate of polymerization by facilitating the deprotonation of the 3'-hydroxyl group in 2-methylimidazole nucleotides (Li et al., 2017) activating the 3'-hydroxyl as a nucleophile. Work by Jin et at., 2018 has shown that Fe^{2+} facilitates RNA primer extension in solutions containing template strands and monomers at a weakly acidic to neutral (pH ~7) optimum while Mg^{2+} is most effective at alkaline conditions (pH ~9). Fe^{2+} could have accordingly enabled an RNA world (as described by Athavale et al., 2012) on Mars, though oxidizing conditions would have favored Mg^{2+} as a catalyst at alkaline conditions as early as ~4.1 Gya. Moreover, for the RNA World to have existed, synthesis (i.e. replication) is at least, if not more important than stability. While degradation in general is slower at weakly acidic pH values, so is template copying chemistry (Jin et at., 2018). Replication with Mg^{2+} as the metal cofactor works best at mildly alkaline pH values, where degradation of RNA is still fairly slow. Fe^{2+} works best as a replication cofactor at neutral to very slightly acidic pH, however, it has severe effects on the stability of RNA and of activated monomers. In other words, replication must be faster than degradation.

Future work is required to further constrain the composition of theoretical Mars waters with respect to mechanisms that may have accumulated metals to prebiotically relevant concentrations (e.g., playas, brines). The work presented here highlights the importance of metals and pH derived from variable bedrock compositions and hypothetical atmospheric conditions on RNA stability. Additional studies will seek to include non-enzymatic RNA extension, the effect of template and complement RNA strands, and additional geological parameters such as UV flux. In summary, the work presented here advances our understanding of

how geochemical environments could have influenced the stability of a potential RNA world on Mars.

5. Conclusions

Discoveries of structural and regulatory RNA molecules suggests that life as we know it may have emerged from an earlier RNA world (Bernhardt, 2012). Subsequently, strides in prebiotic chemistry have demonstrated the synthesis and stability of, and catalysis by, RNA polymers under various conditions and in presence of cofactors (Bernhardt and Tate, 2012). However, it has been challenging to confidently determine the types of real-world environments that may have existed on the Hadean Earth and hosted the origin of life due to global resurfacing and recycling (Marchi et al., 2014). We believe that Mars is the next best alternative to search for environments consistent with requirements imposed by the RNA world. In this study we investigated the influence of bedrock composition (e.g., mafic-ultramafic, iron-rich, magnesium-rich, etc.) and subsequent weathering of prebiotically relevant metals (Fe^{2+}, Mg^{2+}, and Mn^{2+}) on RNA stability. These metals have been demonstrated to catalyze hydrolysis, folding, and enable RNA catalytic activity. In addition, we simultaneously adjusted pH to reflect the composition of hypothetical CO_2-dominated atmospheres in equilibrium with surface waters and an acidic and alkaline vent. We determined that metal-catalyzed hydrolysis of RNA depends on metal concentration and pH. Our results reproduce the enhanced RNA cleavage rates associated with each metal's respective acid dissociation constant (pK_a), and the increase in RNA degradation with increasing metal concentration (Figure 4, Table 1). Meanwhile, degradation rates decreased with increasing metal concentration via an unknown preservation mechanism at pH 3.2 (Figure 3). At pH 9, we encountered Fe^{2+} precipitation which artificially decreased hydrolysis rates while

391 Mn^{2+} precipitation occurred to a lesser extent. We conclude that a Mg^{2+}-rich basalt sourcing
392 metals to slightly acidic (pH 5.4) waters would therefore be the stability optimum (as determined
393 here) for RNA on Mars. However, it is important to note RNA replication chemistry with Mg^{2+}
394 as the metal cofactor requires mildly alkaline pH values (Jin et at., 2018) in order to result in net
395 accumulation. Fortunately, geologic evidence and modeling of basalt weathering indicate that
396 Mars waters would have been near neutral pH ~7. Our experiments at pH 6.7 therefore represent
397 the most accurate interpretation of potentially global conditions on Mars. Results from Fe^{2+} at
398 this pH and prior work on iron catalysis suggest that while high hydrolysis rates lower RNA
399 stability, the presence of Fe^{2+} could have imparted novel catalytic function to candidate
400 ribozymes. However, global oxidizing conditions (due to the lack of a dynamo) on the surface of
401 Mars may have led to significant RNA instability due to the precipitation of RNA-Fe^{3+}
402 complexes in Fe^{2+}-rich environments as early as ~4.1 Gya. We therefore presume the non-redox-
403 sensitive Mg^{2+} would have been a principal catalyst similar to as on the Earth after the great
404 oxidation event. Future Mars exploration should seek to determine the existence and distribution
405 of such predicted environments in order to assess the possible nature and abundance of
406 conditions conducive to an RNA world.
407
408 **Acknowledgements**
409 This work was supported by NASA MatISSE award NNX15AF85G and the MIT Dean of
410 Science Fellowship. We thank Christopher E. Carr and Shui-Ying (Fanny) Ng for helpful input.
411
412 **Author Disclosure Statement**
413 No competing financial interests exist.

References

Adamala, K., Szostak, J.W., 2013. Nonenzymatic Template-Directed RNA Synthesis Inside Model Protocells. Science 342, 1098–1100. https://doi.org/10.1126/science.1241888

Adcock, C.T., Hausrath, E.M., Forster, P.M., 2013. Readily available phosphate from minerals in early aqueous environments on Mars. Nature Geoscience 6, 824–827. https://doi.org/10.1038/ngeo1923

Athavale, S.S., Petrov, A.S., Hsiao, C., Watkins, D., Prickett, C.D., Gossett, J.J., Lie, L., Bowman, J.C., O'Neill, E., Bernier, C.R., Hud, N.V., Wartell, R.M., Harvey, S.C., Williams, L.D., 2012. RNA Folding and Catalysis Mediated by Iron (II). PLOS ONE 7, e38024. https://doi.org/10.1371/journal.pone.0038024

Benner, S.A., Kim, H.-J., 2015. The case for a Martian origin for Earth life, in: Hoover, R.B., Levin, G.V., Rozanov, A.Yu., Wickramasinghe, N.C. (Eds.), . p. 96060C. https://doi.org/10.1117/12.2192890

Bernhardt, H.S., 2012. The RNA world hypothesis: the worst theory of the early evolution of life (except for all the others). Biology Direct 7, 23. https://doi.org/10.1186/1745-6150-7-23

Bernhardt, H.S., Tate, W.P., 2012. Primordial soup or vinaigrette: did the RNA world evolve at acidic pH? Biology Direct 7, 4. https://doi.org/10.1186/1745-6150-7-4

Bibring, J.-P., Langevin, Y., Mustard, J.F., Poulet, F., Arvidson, R., Gendrin, A., Gondet, B., Mangold, N., Pinet, P., Forget, F., the OMEGA team, Berthe, M., Bibring, J.-P., Gendrin, A., Gomez, C., Gondet, B., Jouglet, D., Poulet, F., Soufflot, A., Vincendon, M., Combes, M., Drossart, P., Encrenaz, T., Fouchet, T., Merchiorri, R., Belluci, G., Altieri, F., Formisano, V., Capaccioni, F., Cerroni, P., Coradini, A., Fonti, S., Korablev, O., Kottsov, V., Ignatiev, N., Moroz, V., Titov, D., Zasova, L., Loiseau, D., Mangold, N., Pinet, P., Doute, S., Schmitt, B., Sotin, C., Hauber, E., Hoffmann, H., Jaumann, R., Keller, U., Arvidson, R., Mustard, J.F., Duxbury, T., Forget, F., Neukum, G., 2006. Global Mineralogical and Aqueous Mars History Derived from OMEGA/Mars Express Data. Science 312, 400–404. https://doi.org/10.1126/science.1122659

Boehnke, P., Harrison, T.M., 2016. Illusory Late Heavy Bombardments. Proceedings of the National Academy of Sciences 113, 10802–10806. https://doi.org/10.1073/pnas.1611535113

Bowman, J.C., Lenz, T.K., Hud, N.V., Williams, L.D., 2012. Cations in charge: magnesium ions in RNA folding and catalysis. Current Opinion in Structural Biology 22, 262–272. https://doi.org/10.1016/j.sbi.2012.04.006

Bray, M.S., Lenz, T.K., Haynes, J.W., Bowman, J.C., Petrov, A.S., Reddi, A.R., Hud, N.V., Williams, L.D., Glass, J.B., 2018. Multiple prebiotic metals mediate translation. Proceedings of the National Academy of Sciences 115, 12164–12169. https://doi.org/10.1073/pnas.1803636115

Breaker, R.R., 2012. Riboswitches and the RNA World. Cold Spring Harbor Perspectives in Biology 4, a003566–a003566. https://doi.org/10.1101/cshperspect.a003566

Bura-Nakić, E., Viollier, E., Jézéquel, D., Thiam, A., Ciglenečki, I., 2009. Reduced sulfur and iron species in anoxic water column of meromictic crater Lake Pavin (Massif Central, France). Chemical Geology 266, 311–317. https://doi.org/10.1016/j.chemgeo.2009.06.020

458 Busigny, V., Planavsky, N.J., Jézéquel, D., Crowe, S., Louvat, P., Moureau, J., Viollier, E.,
459 Lyons, T.W., 2014. Iron isotopes in an Archean ocean analogue. Geochimica et
460 Cosmochimica Acta 133, 443–462. https://doi.org/10.1016/j.gca.2014.03.004
461 Callahan, M.P., Smith, K.E., Cleaves, H.J., Ruzicka, J., Stern, J.C., Glavin, D.P., House, C.H.,
462 Dworkin, J.P., 2011. Carbonaceous meteorites contain a wide range of extraterrestrial
463 nucleobases. Proceedings of the National Academy of Sciences 108, 13995–13998.
464 https://doi.org/10.1073/pnas.1106493108
465 Carr, C.E., Mojarro, A., Hachey, J., Saboda, K., Tani, J., Bhattaru, S.A., Smith, A., Pontefract,
466 A., Zuber, M.T., Doebler, R., Brown, M., Herrington, K., Talbot, R., Nguyen, V., Bailey,
467 R., Ferguson, T., Finney, M., Church, G., Ruvkun, G., 2017. Towards in situ sequencing
468 for life detection. IEEE, pp. 1–18. https://doi.org/10.1109/AERO.2017.7943896
469 Catling, D.C., 1999. A chemical model for evaporites on early Mars: Possible sedimentary
470 tracers of the early climate and implications for exploration. Journal of Geophysical
471 Research: Planets 104, 16453–16469. https://doi.org/10.1029/1998JE001020
472 Cech, T.R., 2000. The Ribosome Is a Ribozyme. Science 289, 878–879.
473 https://doi.org/10.1126/science.289.5481.878
474 Cockell, C.S., Catling, D.C., Davis, W.L., Snook, K., Kepner, R.L., Lee, P., McKay, C.P., 2000.
475 The Ultraviolet Environment of Mars: Biological Implications Past, Present, and Future.
476 Icarus 146, 343–359. https://doi.org/10.1006/icar.2000.6393
477 Craddock, R.A., Irwin, R.P., Howard, A.D., 2003. Characteristics of Martian Valley Networks
478 and the Implications for Past Climates. Lunar and Planetary Science Conference 1888.
479 Crick, F., 1970. Central Dogma of Molecular Biology. Nature 227, 561.
480 https://doi.org/10.1038/227561a0
481 Ehlmann, B.L., Mustard, J.F., Murchie, S.L., Bibring, J.-P., Meunier, A., Fraeman, A.A.,
482 Langevin, Y., 2011. Subsurface water and clay mineral formation during the early history
483 of Mars. Nature 479, 53–60. https://doi.org/10.1038/nature10582
484 Ehlmann, B.L., Mustard, J.F., Murchie, S.L., Poulet, F., Bishop, J.L., Brown, A.J., Calvin, W.M.,
485 Clark, R.N., Marais, D.J.D., Milliken, R.E., Roach, L.H., Roush, T.L., Swayze, G.A.,
486 Wray, J.J., 2008. Orbital Identification of Carbonate-Bearing Rocks on Mars. Science
487 322, 1828–1832. https://doi.org/10.1126/science.1164759
488 Fassett, C.I., Head, J.W., 2011. Sequence and timing of conditions on early Mars. Icarus 211,
489 1204–1214. https://doi.org/10.1016/j.icarus.2010.11.014
490 Fassett, C.I., Head, J.W., 2008a. The timing of martian valley network activity: Constraints from
491 buffered crater counting. Icarus 195, 61–89. https://doi.org/10.1016/j.icarus.2007.12.009
492 Fassett, C.I., Head, J.W., 2008b. Valley network-fed, open-basin lakes on Mars: Distribution and
493 implications for Noachian surface and subsurface hydrology. Icarus 198, 37–56.
494 https://doi.org/10.1016/j.icarus.2008.06.016
495 Fedor, M.J., 2002. The role of metal ions in RNA catalysis. Current Opinion in Structural
496 Biology 12, 289–295. https://doi.org/10.1016/S0959-440X(02)00324-X
497 Ferris, J.P., 2006. Montmorillonite-catalysed formation of RNA oligomers: the possible role of
498 catalysis in the origins of life. Philosophical Transactions of the Royal Society B:
499 Biological Sciences 361, 1777–1786. https://doi.org/10.1098/rstb.2006.1903
500 Forget, F., Wordsworth, R., Millour, E., Madeleine, J.-B., Kerber, L., Leconte, J., Marcq, E.,
501 Haberle, R.M., 2013. 3D modelling of the early martian climate under a denser CO2
502 atmosphere: Temperatures and CO2 ice clouds. Icarus 222, 81–99.
503 https://doi.org/10.1016/j.icarus.2012.10.019

Furukawa, Y., Kakegawa, T., 2017. Borate and the Origin of RNA: A Model for the Precursors to Life. Elements 13, 261–265. https://doi.org/10.2138/gselements.13.4.261

Gasda, P.J., Haldeman, E.B., Wiens, R.C., Rapin, W., Bristow, T.F., Bridges, J.C., Schwenzer, S.P., Clark, B., Herkenhoff, K., Frydenvang, J., Lanza, N.L., Maurice, S., Clegg, S., Delapp, D.M., Sanford, V.L., Bodine, M.R., McInroy, R., 2017. In situ detection of boron by ChemCam on Mars: First Detection of Boron on Mars. Geophysical Research Letters 44, 8739–8748. https://doi.org/10.1002/2017GL074480

Gayer, K.H., Woontner, L., 1956. The Solubility of Ferrous Hydroxide and Ferric Hydroxide in Acidic and Basic Media at 25°. The Journal of Physical Chemistry 60, 1569–1571. https://doi.org/10.1021/j150545a021

Gilbert, W., 1986. Origin of life: The RNA world. Nature 319, 618. https://doi.org/10.1038/319618a0

Gladman, B.J., Burns, J.A., Duncan, M., Lee, P., Levison, H.F., 1996. The Exchange of Impact Ejecta Between Terrestrial Planets. Science 271, 1387–1392. https://doi.org/10.1126/science.271.5254.1387

Gomes, R., Levison, H.F., Tsiganis, K., Morbidelli, A., 2005. Origin of the cataclysmic Late Heavy Bombardment period of the terrestrial planets. Nature 435, 466–469. https://doi.org/10.1038/nature03676

Goudge, T.A., Head, J.W., Mustard, J.F., Fassett, C.I., 2012. An analysis of open-basin lake deposits on Mars: Evidence for the nature of associated lacustrine deposits and post-lacustrine modification processes. Icarus 219, 211–229. https://doi.org/10.1016/j.icarus.2012.02.027

Goudge, T.A., Mustard, J.F., Head, J.W., Fassett, C.I., Wiseman, S.M., 2015. Assessing the mineralogy of the watershed and fan deposits of the Jezero crater paleolake system, Mars: Jezero Paleolake System Mineralogy. Journal of Geophysical Research: Planets 120, 775–808. https://doi.org/10.1002/2014JE004782

Grotzinger, J.P., Gupta, S., Malin, M.C., Rubin, D.M., Schieber, J., Siebach, K., Sumner, D.Y., Stack, K.M., Vasavada, A.R., Arvidson, R.E., Calef, F., Edgar, L., Fischer, W.F., Grant, J.A., Griffes, J., Kah, L.C., Lamb, M.P., Lewis, K.W., Mangold, N., Minitti, M.E., Palucis, M., Rice, M., Williams, R.M.E., Yingst, R.A., Blake, D., Blaney, D., Conrad, P., Crisp, J., Dietrich, W.E., Dromart, G., Edgett, K.S., Ewing, R.C., Gellert, R., Hurowitz, J.A., Kocurek, G., Mahaffy, P., McBride, M.J., McLennan, S.M., Mischna, M., Ming, D., Milliken, R., Newsom, H., Oehler, D., Parker, T.J., Vaniman, D., Wiens, R.C., Wilson, S.A., 2015. Deposition, exhumation, and paleoclimate of an ancient lake deposit, Gale crater, Mars. Science 350, aac7575–aac7575. https://doi.org/10.1126/science.aac7575

Grotzinger, J.P., Sumner, D.Y., Kah, L.C., Stack, K., Gupta, S., Edgar, L., Rubin, D., Lewis, K., Schieber, J., Mangold, N., Milliken, R., Conrad, P.G., DesMarais, D., Farmer, J., Siebach, K., McLennan, S.M., Ming, D., Vaniman, D., Crisp, J., Vasavada, A., Edgett, K.S., Malin, M., Blake, D., Gellert, R., Mahaffy, P., Wiens, R.C., Maurice, S., Grant, J.A., Wilson, S., Anderson, R.C., Beegle, L., Arvidson, R., Hallet, B., Sletten, R.S., Rice, M., Bell, J., Griffes, J., Ehlmann, B., Anderson, R.B., Bristow, T.F., Dietrich, W.E., Eigenbrode, J., Hardgrove, C., Herkenhoff, K., Jandura, L., Kocurek, G., Lee, S., Leshin, L.A., Leveille, R., Limonadi, D., Maki, J., McCloskey, S., Meyer, M., Minitti, M., Newsom, H., Oehler, D., Okon, A., Palucis, M., Parker, T., Rowland, S., Schmidt, M., Squyres, S., Steele, A., Stolper, E., Summons, R., Treiman, A., Yingst, A., MSL Team,

2014. A Habitable Fluvio-Lacustrine Environment at Yellowknife Bay, Gale Crater, Mars. Science 343, 1242777–1242777. https://doi.org/10.1126/science.1242777

Halevy, I., Bachan, A., 2017. The geologic history of seawater pH. Science 355, 1069–1071. https://doi.org/10.1126/science.aal4151

Halevy, I., Head III, J.W., 2014. Episodic warming of early Mars by punctuated volcanism. Nature Geoscience 7, 865–868. https://doi.org/10.1038/ngeo2293

Hampel, A., Cowan, J.A., 1997. A unique mechanism for RNA catalysis: the role of metal cofactors in hairpin ribozyme cleavage. Chemistry & Biology 4, 513–517. https://doi.org/10.1016/S1074-5521(97)90323-9

Hartmann, W.K., Neukum, G., 2001. Cratering Chronology and the Evolution of Mars, in: Kallenbach, R., Geiss, J., Hartmann, W.K. (Eds.), Chronology and Evolution of Mars, Space Sciences Series of ISSI. Springer Netherlands, pp. 165–194.

Head, J.W., Marchant, D.R., 2014. The climate history of early Mars: insights from the Antarctic McMurdo Dry Valleys hydrologic system. Antarctic Science 26, 774–800. https://doi.org/10.1017/S0954102014000686

Hernández-Morales, R., Becerra, A., Lazcano, A., 2019. Alarmones as Vestiges of a Bygone RNA World. Journal of Molecular Evolution 87, 37–51. https://doi.org/10.1007/s00239-018-9883-3

Hongve, D., 1994. Nutrient metabolism (C, N, P, and Si) in the trophogenic zone of a meromictic lake. Hydrobiologia 277, 17–39. https://doi.org/10.1007/BF00023983

Hsiao, C., Chou, I.-C., Okafor, C.D., Bowman, J.C., O'Neill, E.B., Athavale, S.S., Petrov, A.S., Hud, N.V., Wartell, R.M., Harvey, S.C., Williams, L.D., 2013. RNA with iron(II) as a cofactor catalyses electron transfer. Nature Chemistry 5, 525–528. https://doi.org/10.1038/nchem.1649

Hurowitz, J.A., Fischer, W.W., Tosca, N.J., Milliken, R.E., 2010. Origin of acidic surface waters and the evolution of atmospheric chemistry on early Mars. Nature Geoscience 3, 323–326. https://doi.org/10.1038/ngeo831

Hurowitz, J.A., Grotzinger, J.P., Fischer, W.W., McLennan, S.M., Milliken, R.E., Stein, N., Vasavada, A.R., Blake, D.F., Dehouck, E., Eigenbrode, J.L., Fairén, A.G., Frydenvang, J., Gellert, R., Grant, J.A., Gupta, S., Herkenhoff, K.E., Ming, D.W., Rampe, E.B., Schmidt, M.E., Siebach, K.L., Stack-Morgan, K., Sumner, D.Y., Wiens, R.C., 2017. Redox stratification of an ancient lake in Gale crater, Mars. Science 356, eaah6849. https://doi.org/10.1126/science.aah6849

Hynek, B.M., Beach, M., Hoke, M.R.T., 2010. Updated global map of Martian valley networks and implications for climate and hydrologic processes. Journal of Geophysical Research: Planets 115. https://doi.org/10.1029/2009JE003548

Jackson, V.E., Felmy, A.R., Dixon, D.A., 2015. Prediction of the pKa's of Aqueous Metal Ion +2 Complexes. J. Phys. Chem. A 119, 2926–2939. https://doi.org/10.1021/jp5118272

Jakosky, B.M., Slipski, M., Benna, M., Mahaffy, P., Elrod, M., Yelle, R., Stone, S., Alsaeed, N., 2017. Mars' atmospheric history derived from upper-atmosphere measurements of 38Ar/36Ar. Science 355, 1408–1410. https://doi.org/10.1126/science.aai7721

Jimenez, J.I., Xulvi-Brunet, R., Campbell, G.W., Turk-MacLeod, R., Chen, I.A., 2013. Comprehensive experimental fitness landscape and evolutionary network for small RNA. Proceedings of the National Academy of Sciences 110, 14984–14989. https://doi.org/10.1073/pnas.1307604110

Jin, L., Engelhart, A.E., Zhang, W., Adamala, K., Szostak, J.W., 2018. Catalysis of Template-Directed Nonenzymatic RNA Copying by Iron(II). Journal of the American Chemical Society 140, 15016–15021. https://doi.org/10.1021/jacs.8b09617

Johnson-Buck, A.E., McDowell, S.E., Walter, N.G., 2011. Metal Ions: Supporting Actors in the Playbook of Small Ribozymes. Met Ions Life Sci 9, 175–196.

Joyce, G.F., Szostak, J.W., 2018. Protocells and RNA Self-Replication. Cold Spring Harbor Perspectives in Biology 10, a034801. https://doi.org/10.1101/cshperspect.a034801

Kling, G.W., Tuttle, M.L., Evans, W.C., 1989. The evolution of thermal structure and water chemistry in Lake Nyos. Journal of Volcanology and Geothermal Research 39, 151–165. https://doi.org/10.1016/0377-0273(89)90055-3

Klingelhofer, G., 2004. Jarosite and Hematite at Meridiani Planum from Opportunity's Mossbauer Spectrometer. Science 306, 1740–1745. https://doi.org/10.1126/science.1104653

Krissansen-Totton, J., Arney, G.N., Catling, D.C., 2018. Constraining the climate and ocean pH of the early Earth with a geological carbon cycle model. Proceedings of the National Academy of Sciences 115, 4105–4110. https://doi.org/10.1073/pnas.1721296115

Kua, J., Bada, J.L., 2011. Primordial Ocean Chemistry and its Compatibility with the RNA World. Origins of Life and Evolution of Biospheres 41, 553–558. https://doi.org/10.1007/s11084-011-9250-5

Laing, L.G., Gluick, T.C., Draper, D.E., 1994. Stabilization of RNA Structure by Mg Ions: Specific and Non-specific Effects. Journal of Molecular Biology 237, 577–587. https://doi.org/10.1006/jmbi.1994.1256

Lanza, N.L., Wiens, R.C., Arvidson, R.E., Clark, B.C., Fischer, W.W., Gellert, R., Grotzinger, J.P., Hurowitz, J.A., McLennan, S.M., Morris, R.V., Rice, M.S., Bell, J.F., Berger, J.A., Blaney, D.L., Bridges, N.T., Calef, F., Campbell, J.L., Clegg, S.M., Cousin, A., Edgett, K.S., Fabre, C., Fisk, M.R., Forni, O., Frydenvang, J., Hardy, K.R., Hardgrove, C., Johnson, J.R., Lasue, J., Le Mouélic, S., Malin, M.C., Mangold, N., Martìn-Torres, J., Maurice, S., McBride, M.J., Ming, D.W., Newsom, H.E., Ollila, A.M., Sautter, V., Schröder, S., Thompson, L.M., Treiman, A.H., VanBommel, S., Vaniman, D.T., Zorzano, M.-P., 2016. Oxidation of manganese in an ancient aquifer, Kimberley formation, Gale crater, Mars: Manganese Fracture Fills in Gale Crater. Geophysical Research Letters 43, 7398–7407. https://doi.org/10.1002/2016GL069109

Levy, M., Miller, S.L., 1998. The stability of the RNA bases: Implications for the origin of life. Proceedings of the National Academy of Sciences 95, 7933–7938. https://doi.org/10.1073/pnas.95.14.7933

Li, L., Prywes, N., Tam, C.P., O'Flaherty, D.K., Lelyveld, V.S., Izgu, E.C., Pal, A., Szostak, J.W., 2017. Enhanced Nonenzymatic RNA Copying with 2-Aminoimidazole Activated Nucleotides. Journal of the American Chemical Society 139, 1810–1813. https://doi.org/10.1021/jacs.6b13148

Li, Y., Breaker, R.R., 1999. Kinetics of RNA Degradation by Specific Base Catalysis of Transesterification Involving the 2'-Hydroxyl Group. J. Am. Chem. Soc. 121, 5364–5372. https://doi.org/10.1021/ja990592p

Lillis, R.J., Robbins, S., Manga, M., Halekas, J.S., Frey, H.V., 2013. Time history of the Martian dynamo from crater magnetic field analysis. Journal of Geophysical Research: Planets 1488–1511. https://doi.org/10.1002/jgre.20105@10.1002/(ISSN)2169-9100.EARLYMARS3

Marchi, S., Bottke, W.F., Elkins-Tanton, L.T., Bierhaus, M., Wuennemann, K., Morbidelli, A., Kring, D.A., 2014. Widespread mixing and burial of Earth's Hadean crust by asteroid impacts. Nature 511, 578–582. https://doi.org/10.1038/nature13539

McLennan, S.M., 2012. Geochemistry of Sedimentary Processes on Mars, in: Grotzinger, J.P., Milliken, R.E. (Eds.), Sedimentary Geology of Mars. SEPM Society for Sedimentary Geology, p. 0. https://doi.org/10.2110/pec.12.102.0119

McLennan, S.M., Grotzinger, J.P., Hurowitz, J.A., Tosca, N.J., 2019. The Sedimentary Cycle on Early Mars. Annual Review of Earth and Planetary Sciences 47. https://doi.org/10.1146/annurev-earth-053018-060332

McSween, H.Y., 2002. The rocks of Mars, from far and near. Meteoritics & Planetary Science 37, 7–25. https://doi.org/10.1111/j.1945-5100.2002.tb00793.x

Ming, D.W., Gellert, R., Morris, R.V., Arvidson, R.E., Brückner, J., Clark, B.C., Cohen, B.A., d'Uston, C., Economou, T., Fleischer, I., Klingelhöfer, G., McCoy, T.J., Mittlefehldt, D.W., Schmidt, M.E., Schröder, C., Squyres, S.W., Tréguier, E., Yen, A.S., Zipfel, J., 2008. Geochemical properties of rocks and soils in Gusev Crater, Mars: Results of the Alpha Particle X-Ray Spectrometer from Cumberland Ridge to Home Plate. Journal of Geophysical Research 113. https://doi.org/10.1029/2008JE003195

Mittlefehldt, D.W., 1994. ALH84001, a cumulate orthopyroxenite member of the martian meteorite clan. Meteoritics 29, 214–221. https://doi.org/10.1111/j.1945-5100.1994.tb00673.x

Mojarro, A., Hachey, J., Bailey, R., Brown, M., Doebler, R., Ruvkun, G., Zuber, M.T., Carr, C.E., 2019. Nucleic Acid Extraction and Sequencing from Low-Biomass Synthetic Mars Analog Soils for In Situ Life Detection. Astrobiology. https://doi.org/10.1089/ast.2018.1929

Monteux, J., Andrault, D., Samuel, H., 2016. On the cooling of a deep terrestrial magma ocean. Earth and Planetary Science Letters 448, 140–149. https://doi.org/10.1016/j.epsl.2016.05.010

Moulton, V., Gardner, P.P., Pointon, R.F., Creamer, L.K., Jameson, G.B., Penny, D., 2000. RNA Folding Argues Against a Hot-Start Origin of Life. Journal of Molecular Evolution 51, 416–421. https://doi.org/10.1007/s002390010104

Mustard, J.F., Poulet, F., Gendrin, A., Bibring, J.-P., Langevin, Y., Gondet, B., Mangold, N., Bellucci, G., Altieri, F., 2005. Olivine and Pyroxene Diversity in the Crust of Mars. Science 307, 1594–1597. https://doi.org/10.1126/science.1109098

Nisbet, E.G., Sleep, N.H., 2001. The habitat and nature of early life. Nature 409, 1083–1091. https://doi.org/10.1038/35059210

Nutman, A.P., Bennett, V.C., Friend, C.R.L., Van Kranendonk, M.J., Chivas, A.R., 2016. Rapid emergence of life shown by discovery of 3,700-million-year-old microbial structures. Nature 537, 535–538. https://doi.org/10.1038/nature19355

Oivanen, M., Kuusela, S., Lönnberg, H., 1998. Kinetics and Mechanisms for the Cleavage and Isomerization of the Phosphodiester Bonds of RNA by Brønsted Acids and Bases. Chemical Reviews 98, 961–990. https://doi.org/10.1021/cr960425x

Okafor, C.D., Lanier, K.A., Petrov, A.S., Athavale, S.S., Bowman, J.C., Hud, N.V., Williams, L.D., 2017. Iron mediates catalysis of nucleic acid processing enzymes: support for Fe(II) as a cofactor before the great oxidation event. Nucleic Acids Research 45, 3634–3642. https://doi.org/10.1093/nar/gkx171

685 Palumbo, A.M., Head, J.W., 2018. Impact cratering as a cause of climate change, surface
686 alteration, and resurfacing during the early history of Mars. Meteoritics & Planetary
687 Science 53, 687–725. https://doi.org/10.1111/maps.13001
688 Palumbo, A.M., Head, J.W., Wordsworth, R.D., 2018. Late Noachian Icy Highlands climate
689 model: Exploring the possibility of transient melting and fluvial/lacustrine activity
690 through peak annual and seasonal temperatures. Icarus 300, 261–286.
691 https://doi.org/10.1016/j.icarus.2017.09.007
692 Patel, B.H., Percivalle, C., Ritson, D.J., Duffy, C.D., Sutherland, J.D., 2015. Common origins of
693 RNA, protein and lipid precursors in a cyanosulfidic protometabolism. Nature Chemistry
694 7, 301–307. https://doi.org/10.1038/nchem.2202
695 Petrov, A.S., Bernier, C.R., Hsiao, C., Okafor, C.D., Tannenbaum, E., Stern, J., Gaucher, E.,
696 Schneider, D., Hud, N.V., Harvey, S.C., Dean Williams, L., 2012. RNA–Magnesium–
697 Protein Interactions in Large Ribosomal Subunit. The Journal of Physical Chemistry B
698 116, 8113–8120. https://doi.org/10.1021/jp304723w
699 Petrov, A.S., Gulen, B., Norris, A.M., Kovacs, N.A., Bernier, C.R., Lanier, K.A., Fox, G.E.,
700 Harvey, S.C., Wartell, R.M., Hud, N.V., Williams, L.D., 2015. History of the ribosome
701 and the origin of translation. Proceedings of the National Academy of Sciences 112,
702 15396–15401. https://doi.org/10.1073/pnas.1509761112
703 Powner, M.W., Gerland, B., Sutherland, J.D., 2009. Synthesis of activated pyrimidine
704 ribonucleotides in prebiotically plausible conditions. Nature 459, 239–242.
705 https://doi.org/10.1038/nature08013
706 Ritson, D.J., Battilocchio, C., Ley, S.V., Sutherland, J.D., 2018. Mimicking the surface and
707 prebiotic chemistry of early Earth using flow chemistry. Nature Communications 9.
708 https://doi.org/10.1038/s41467-018-04147-2
709 Runnels, C.M., Lanier, K.A., Williams, J.K., Bowman, J.C., Petrov, A.S., Hud, N.V., Williams,
710 L.D., 2018. Folding, Assembly, and Persistence: The Essential Nature and Origins of
711 Biopolymers. Journal of Molecular Evolution 86, 598–610.
712 https://doi.org/10.1007/s00239-018-9876-2
713 Schrum, J.P., Zhu, T.F., Szostak, J.W., 2010. The Origins of Cellular Life. Cold Spring Harbor
714 Perspectives in Biology 2, a002212–a002212.
715 https://doi.org/10.1101/cshperspect.a002212
716 Segura, T.L., Toon, O.B., Colaprete, A., 2008. Modeling the environmental effects of moderate-
717 sized impacts on Mars. Journal of Geophysical Research: Planets 113.
718 https://doi.org/10.1029/2008JE003147
719 Squyres, S.W., Knoll, A.H., 2005. Sedimentary rocks at Meridiani Planum: Origin, diagenesis,
720 and implications for life on Mars. Earth and Planetary Science Letters 240, 1–10.
721 https://doi.org/10.1016/j.epsl.2005.09.038
722 Squyres, S.W., Knoll, A.H., Arvidson, R.E., Clark, B.C., Grotzinger, J.P., Jolliff, B.L.,
723 McLennan, S.M., Tosca, N., Bell, J.F., Calvin, W.M., Farrand, W.H., Glotch, T.D.,
724 Golombek, M.P., Herkenhoff, K.E., Johnson, J.R., Klingelhofer, G., McSween, H.Y.,
725 Yen, A.S., 2006. Two Years at Meridiani Planum: Results from the Opportunity Rover.
726 Science 313, 1403–1407. https://doi.org/10.1126/science.1130890
727 Steakley, K., Murphy, J., Kahre, M., Haberle, R., Kling, A., 2019. Testing the impact heating
728 hypothesis for early Mars with a 3-D global climate model. Icarus 330, 169–188.
729 https://doi.org/10.1016/j.icarus.2019.04.005

Szostak, J.W., 2012. The eightfold path to non-enzymatic RNA replication. J Syst Chem 3, 2. https://doi.org/10.1186/1759-2208-3-2

Tarnas, J.D., Mustard, J.F., Sherwood Lollar, B., Bramble, M.S., Cannon, K.M., Palumbo, A.M., Plesa, A.-C., 2018. Radiolytic H2 production on Noachian Mars: Implications for habitability and atmospheric warming. Earth and Planetary Science Letters 502, 133–145. https://doi.org/10.1016/j.epsl.2018.09.001

Tian, F., Claire, M.W., Haqq-Misra, J.D., Smith, M., Crisp, D.C., Catling, D., Zahnle, K., Kasting, J.F., 2010. Photochemical and climate consequences of sulfur outgassing on early Mars. Earth and Planetary Science Letters 295, 412–418. https://doi.org/10.1016/j.epsl.2010.04.016

Turbet, M., Gillmann, C., Forget, F., Baudin, B., Palumbo, A., Head, J., Karatekin, O., 2020. The environmental effects of very large bolide impacts on early Mars explored with a hierarchy of numerical models. Icarus 335, 113419. https://doi.org/10.1016/j.icarus.2019.113419

van Roode, J.H.G., Orgel, L.E., 1980. Template-directed synthesis of oligoguanylates in the presence of metal ions. Journal of Molecular Biology 144, 579–585. https://doi.org/10.1016/0022-2836(80)90338-1

Voytek, S.B., Joyce, G.F., 2007. Emergence of a fast-reacting ribozyme that is capable of undergoing continuous evolution. PNAS 104, 15288–15293. https://doi.org/10.1073/pnas.0707490104

Weiss, B.P., 2000. A Low Temperature Transfer of ALH84001 from Mars to Earth. Science 290, 791–795. https://doi.org/10.1126/science.290.5492.791

Wordsworth, R., Forget, F., Millour, E., Head, J.W., Madeleine, J.-B., Charnay, B., 2013. Global modelling of the early martian climate under a denser CO2 atmosphere: Water cycle and ice evolution. Icarus 222, 1–19. https://doi.org/10.1016/j.icarus.2012.09.036

Wordsworth, R., Kalugina, Y., Lokshtanov, S., Vigasin, A., Ehlmann, B., Head, J., Sanders, C., Wang, H., 2017. Transient reducing greenhouse warming on early Mars. Geophysical Research Letters 44, 665–671. https://doi.org/10.1002/2016GL071766

Yen, A.S., Morris, R.V., Clark, B.C., Gellert, R., Knudson, A.T., Squyres, S., Mittlefehldt, D.W., Ming, D.W., Arvidson, R., McCoy, T., Schmidt, M., Hurowitz, J., Li, R., Johnson, J.R., 2008. Hydrothermal processes at Gusev Crater: An evaluation of Paso Robles class soils. Journal of Geophysical Research 113. https://doi.org/10.1029/2007JE002978

Figure 1: *Oligonucleotide cleavage assay*. A hybrid RNA-DNA oligomer, 5'-Cy3-TTT-TTT-rCTT-TTT-TTT-3', was designed to contain a single ribonucletide (r) in between a chain of deoxyribonucleotides which could allow us to quantify cleavage at a single site. Representative gel scan displays two bands belonging to either the intact 15-mer (Band 1) or the residual 7-mer (Band 2) cleaved at the single ribonucleotide site.

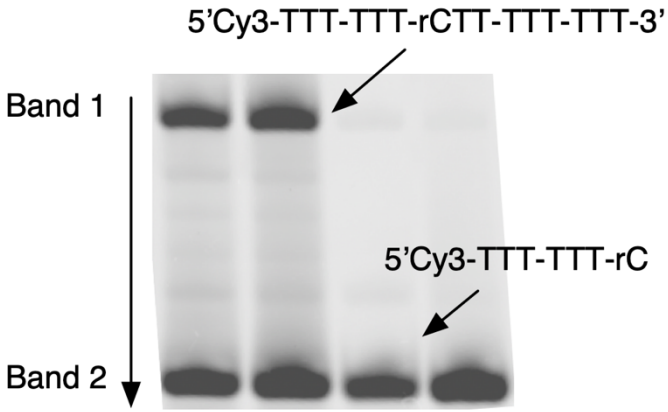

Figure 2: *Metal ion catalysis of RNA degradation.* Plot of oligonucleotide strand cleavage at the site of an RNA nucleotide as measured by urea polyacrylamide gel electrophoresis with 50 mM Fe^{2+} (●), 50 mM Mg^{2+} (▲), and 50 mM Mn^{2+} (■) at pH 6.7. The natural logarithm of the fraction of un-cleaved RNA with time (h) was fit to a linear regression $\ln[p_t] = -kt + \ln[p_o]$ and the slope yielded our pseudo-first-order rate constants ($k_{obs}(h^{-1})$).

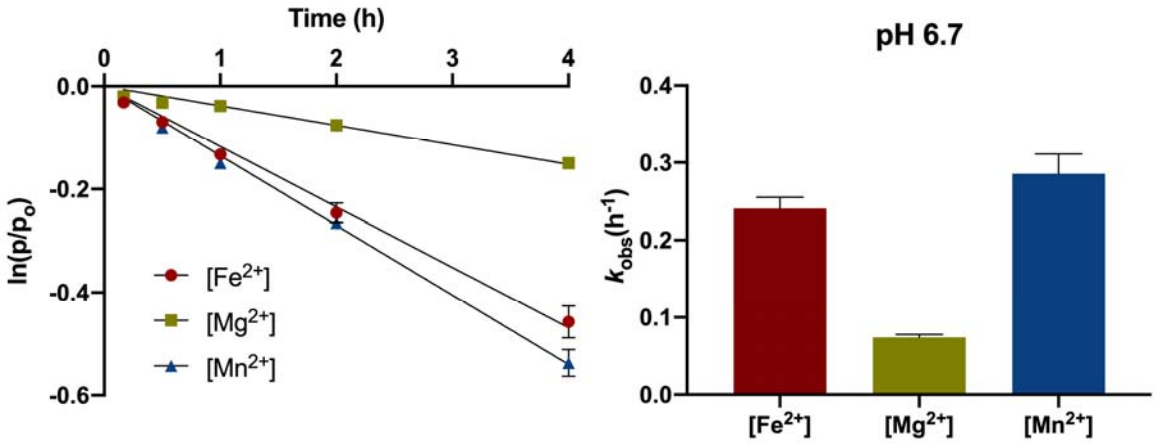

Figure 3: *RNA degradation at pH 3.2*. Incubation of the chimeric RNA-DNA oligonucleotide at pH 3.2 indicates that increasing concentrations of prebiotic metals decrease the rate of RNA degradation. RNA degradation is best mitigated by Mg^{2+} at 50 mM (k_{obs} = 0.013), compared to Fe^{2+} at 50 mM (k_{obs} = 0.025), Mn^{2+} at 50 mM (k_{obs} = 0.026) and the no divalent metal cation negative control (k_{obs} = 0.081). Error bars represent S.E.M. (n = 2).

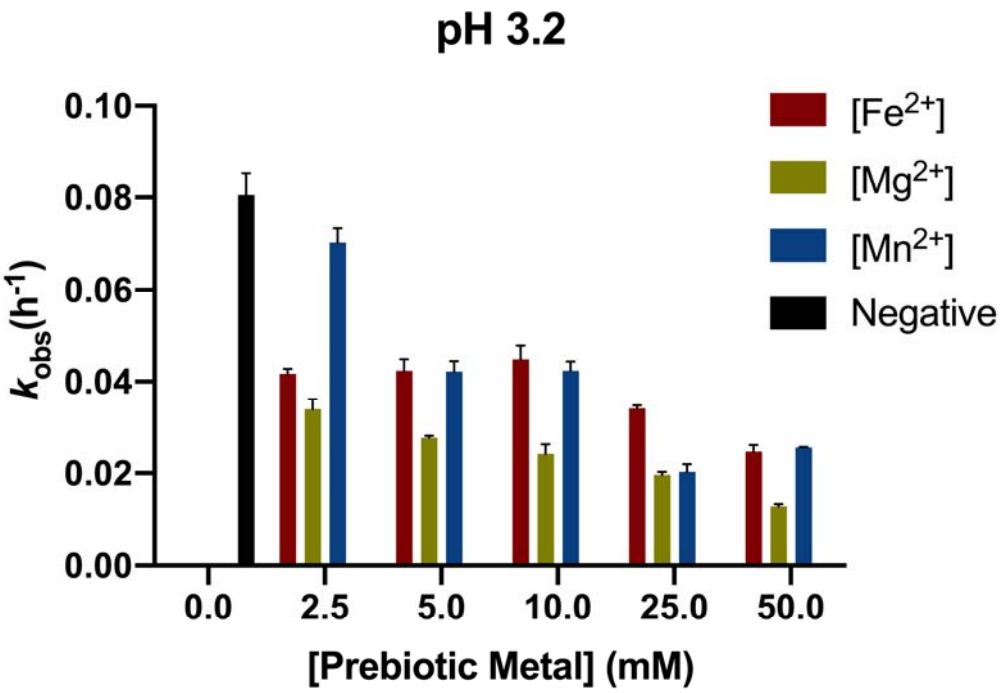

825 **Figure 4:** *Characterization of RNA degradation kinetics.* Saturation curves of Fe^{2+} and Mg^{2+}
826 metal-catalyzed hydrolysis fitted to the Michaelis-Menten equation for enzyme kinetics. Within
827 the range tested, we observe greater RNA stability at pH 5.4 where the maximum rate of
828 hydrolysis (k_{max}) with Mg^{2+} is lower than with Fe^{2+}. RNA degradation experiments with Fe^{2+} at
829 pH 6.7 did not reach saturation. Error bars represent S.E.M. (n=2).
830

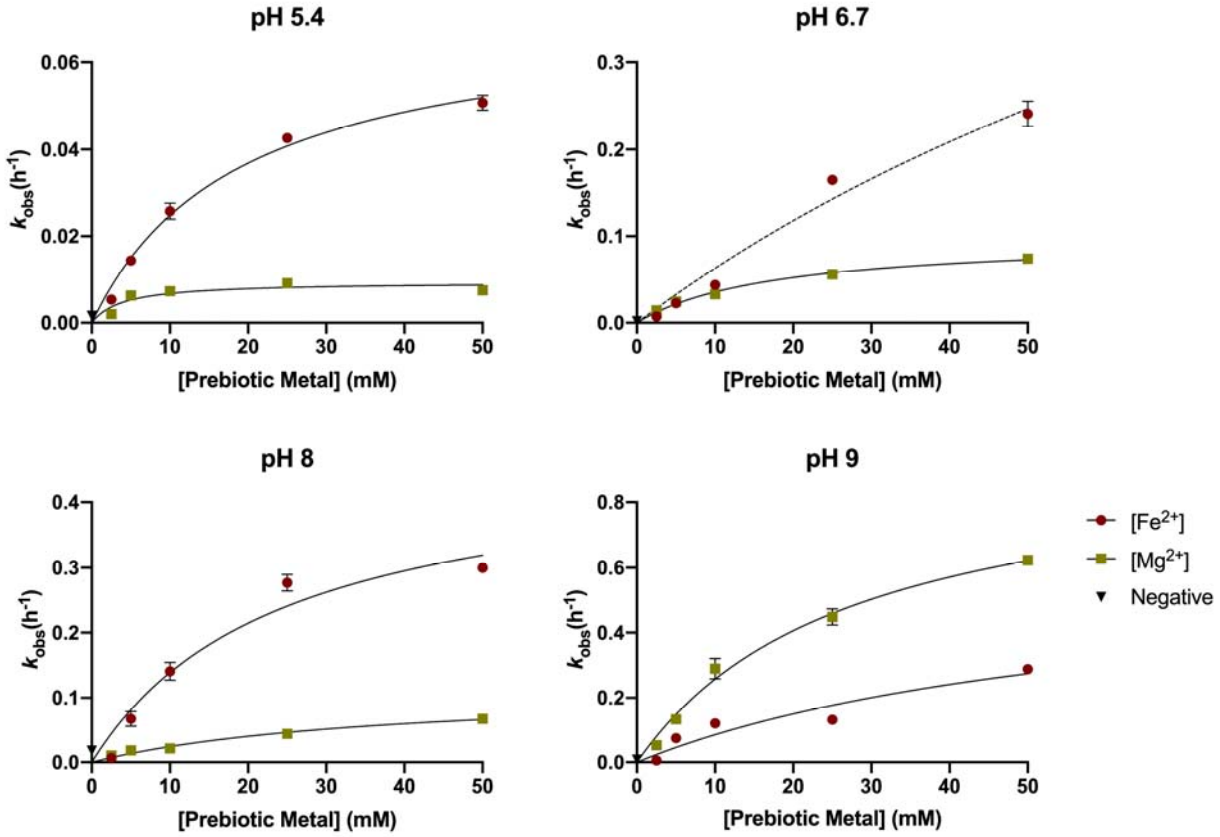

831
832
833
834
835
836

837 **Figure 5:** *Manganese-catalyzed RNA degradation.* Trends for Mn^{2+} are qualitatively similar to
838 Fe^{2+} between pH 3.2 and 8. At pH 9 however, substantially more Fe^{2+} was observed to
839 precipitate out of solution versus Mn^{2+}. Error bars represent S.E.M. (n=2).
840

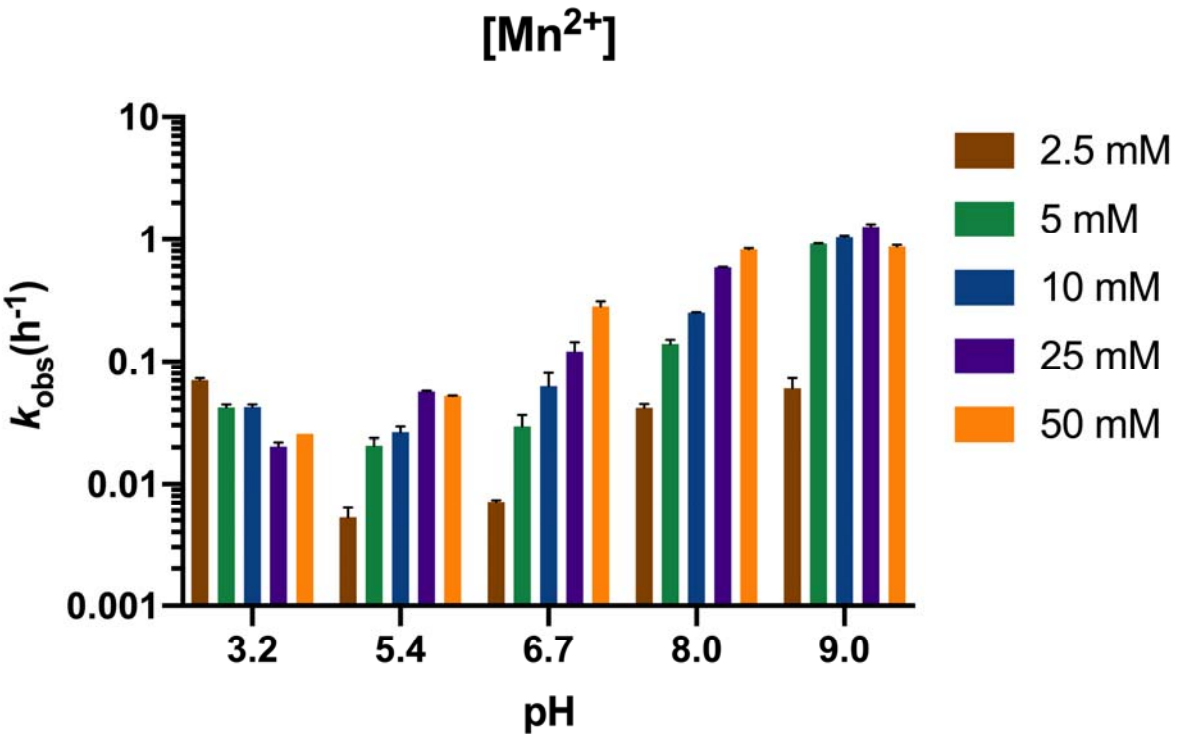

841
842
843
844
845
846
847
848

Figure 6: *Prebiotic metal mixture-catalyzed RNA degradation.* Results for the basalt analog solutions tend towards less overall metal-catalyzed hydrolysis in Mg^{2+}-rich solutions (e.g., forsteritic) over Fe^{2+}-rich solutions (e.g., fayalitic). Metal-catalyzed degradation at pH 9 for all basalt analogs is inferred to be primarily Mg^{2+}-dominated as Fe^{2+} was observed to precipitate out of solution after 24 hours. Error bars represent S.E.M. (n=2).

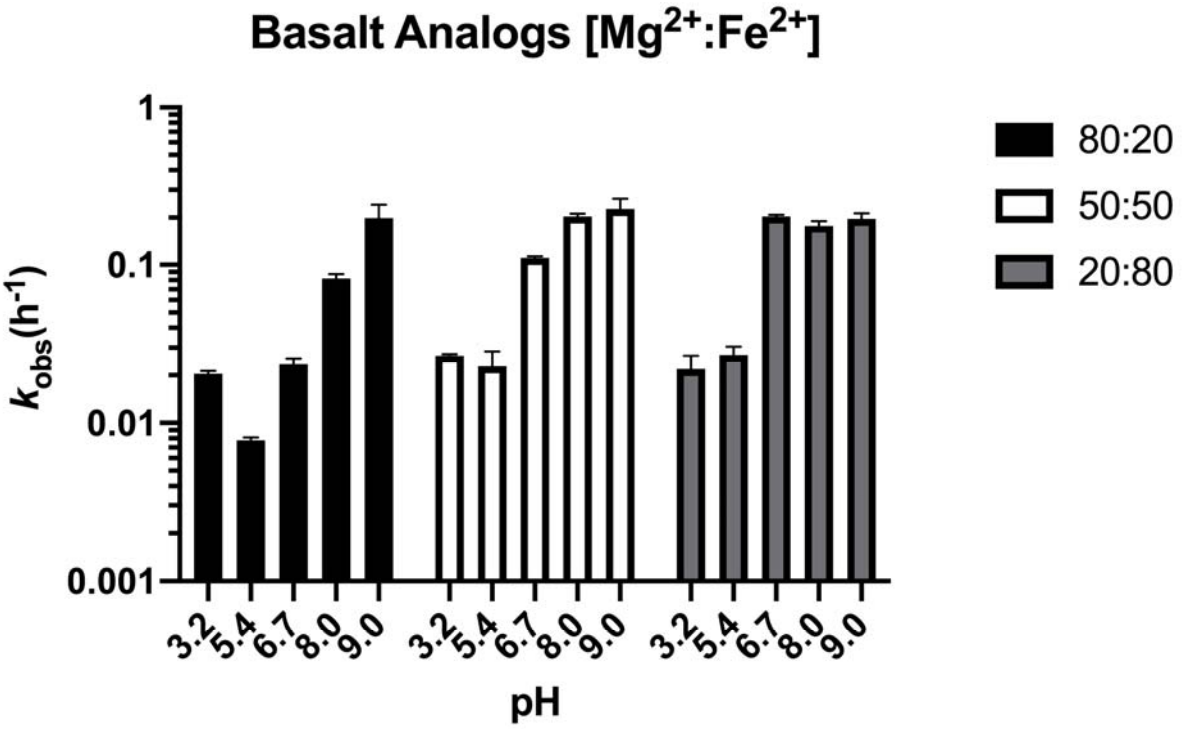

Table 1	**pH 3.2**			**pH 5.4**			**pH 6.7**			**pH 8**			**pH 9**		
Metal	$\boldsymbol{k_{obs}}$ **(h^{-1}) (10^{-2})**	**S.E.M. (10^{-3})**	**$t_{1/2}$ (h)**	$\boldsymbol{k_{obs}}$ **(h^{-1}) (10^{-2})**	**S.E.M. (10^{-3})**	**$t_{1/2}$ (h)**	$\boldsymbol{k_{obs}}$ **(h^{-1}) (10^{-2})**	**S.E.M. (10^{-3})**	**$t_{1/2}$ (h)**	$\boldsymbol{k_{obs}}$ **(h^{-1}) (10^{-2})**	**S.E.M. (10^{-3})**	**$t_{1/2}$ (h)**	$\boldsymbol{k_{obs}}$ **(h^{-1}) (10^{-2})**	**S.E.M. (10^{-3})**	**$t_{1/2}$ (h)**
[Fe^{2+}]															
50 mM	2.47	1.40	28	5.07	1.70	14	24.1	14.5	3	30.0	6.10	2	28.9	13.2	2
25 mM	3.41	0.70	20	4.26	0.50	16	16.5	1.30	4	27.7	12.6	3	13.3	2.65	5
10 mM	4.49	3.05	15	2.58	1.85	27	4.40	3.65	16	14.1	13.8	5	12.1	5.50	6
5 mM	4.24	2.55	16	1.44	0.95	48	2.26	2.75	31	6.76	11.3	10	7.48	1.20	9
2.5 mM	4.17	1.10	17	0.54	0.25	130	0.74	3.80	94	0.65	0.25	107	5.40	7.00	13
[Mg^{2+}]															
50 mM	1.28	0.50	54	0.75	0.70	92	7.42	3.75	9	6.76	0.30	10	62.3	11.3	1
25 mM	1.97	0.65	35	0.92	0.05	76	5.61	1.45	12	4.41	3.00	16	44.9	25.1	2
10 mM	2.43	2.05	29	0.73	0.10	95	3.31	1.30	21	2.16	0.70	32	29.0	31.2	2
5 mM	2.77	0.40	25	0.63	0.40	110	2.46	1.45	28	1.85	6.10	37	13.4	13.9	5
2.5 mM	3.40	2.15	20	0.20	0.10	347	1.44	3.20	48	1.06	4.10	65	5.32	0.60	13
[Mn^{2+}]															
50 mM	2.57	0.05	27	5.22	0.35	13	28.6	25.5	2	82.7	20.7	1	87.5	29.9	1
25 mM	2.03	1.70	34	5.68	0.80	12	12.2	24.1	6	58.9	9.05	1	127	62.1	1
10 mM	4.24	2.00	16	2.64	2.90	26	6.29	18.0	11	25.4	3.10	3	104	27.9	1
5 mM	4.22	2.28	16	2.07	3.10	33	2.95	6.95	24	14.1	11.0	5	92.2	4.65	1
2.5 mM	7.03	3.10	10	0.53	1.10	131	0.72	0.25	97	4.20	3.00	17	6.04	12.9	11
Basalt Analogs [Mg^{2+}:Fe^{2+}]															
80:20	2.05	0.65	34	0.78	0.20	89	2.35	1.50	29	8.20	3.70	8	19.9	30.3	3
50:50	2.68	0.35	26	2.29	3.95	30	11.1	1.75	6	20.4	6.05	3	22.8	25.4	3
20:80	2.20	3.30	32	2.70	2.40	26	20.3	3.85	3	17.7	9.30	4	19.7	11.2	4
Negative Control															
0 mM	8.06	4.85	9	0.16	0.70	433	0.20	0.15	355	1.82	1.30	38	0.81	1.10	86

Table 2

Metal	pH	k_{max} (h^{-1}) (10^{-2})	S.E.M. (10^{-3})	Km	S.E.M.
[Fe^{2+}]	5.4	7.14	4.46	18.8	2.74
	6.7	90.9	469	134	89.7
	8	47.3	73.3	24.1	8.03
	9	47.4	147	38.7	22.1
[Mg^{2+}]	5.4	0.95	0.99	3.97	1.59
	6.7	9.86	6.47	17.7	2.77
	8	11.7	21.1	37.8	12.7
	9	96.1	86.2	27.3	5.06

871